Magnetic and structural phase diagram of $Tb_5(Si_xGe_{1-x})_4$

C. Ritter
Institut Laue-Langevin, Boîte Postale 156, 38042 Grenoble Cédex 9, France

L. Morellon,* P. A. Algarabel, C. Magen, and M. R. Ibarra
Departamento de Física de la Materia Condensada and Instituto de Ciencia de Materiales de Aragón, Universidad de Zaragoza and Consejo Superior de Investigaciones Científicas, 50009 Zaragoza, Spain
(Received 7 June 2001; revised manuscript received 24 August 2001; published 1 February 2002)

The different magnetic and crystallographic structures in the series of $Tb_5(Si_xGe_{1-x})_4$ compounds have been studied by means of macroscopic (ac magnetic susceptibility, linear thermal expansion, and resistivity) and microscopic neutron powder diffraction experiments. As a result, the magnetic-crystallographic temperature-composition phase diagram has been determined over the whole temperature range (2–300 K). We have described in detail the origin of the low-temperature magnetic transitions in pure Tb_5Ge_4 and Tb_5Si_4 alloys. Compounds with $x=0.4$, 0.5, and 0.6 present a monoclinic ($P112_1/a$) structure at room temperature. On cooling down, these materials exhibit a first-order crystallographic-magnetic transformation to an orthorhombic (*Pnma*) canted-ferromagnetic structure. These results constitute an experimental evidence of the strong coupling between crystallographic and magnetic degrees of freedom in the $Tb_5(Si_xGe_{1-x})_4$ compounds.

DOI: 10.1103/PhysRevB.65.094405 PACS number(s): 75.25.+z, 75.30.Kz, 75.50.Cc

I. INTRODUCTION

The intimate relationship between crystallography and magnetism has made the $Gd_5(Si_xGe_{1-x})_4$ pseudobinary alloys a unique system where an intriguing and unusual behavior has been found.[1–8] The discovery of the giant magnetocaloric effect (MCE) in the composition range $x \leqslant 0.5$[1,2] triggered a subsequent active research of the crystallographic, magnetic, and transport properties of these exciting materials. In the composition range $0.24 \leqslant x \leqslant 0.5$, the MCE is related to a first-order structural phase transition from a high-temperature monoclinic (paramagnetic) to a low-temperature orthorhombic (ferromagnetic) structure.[3,4] The alloys with $x \leqslant 0.2$ experience on cooling a similar first-order magnetostructural transformation between two different orthorhombic states.[5] In both cases, these transitions can be induced reversibly by applying an external magnetic field, resulting in strong magnetoelastic[3,5] and giant magnetoresistive[6,7] effects. Therefore, this family of compounds is attractive for its potential applications as magnetic refrigerants and/or magnetostrictive and magnetoresistive transducers. Recently, other exciting electrical effects have been reported.[8]

The physical properties of the other lanthanide 5:4 compounds have been explored to a much less extent. Some recent results have been reported by Gschneidner *et al.*[9] on the $R_5(Si_xGe_{1-x})_4$ pseudobinary system with $R=$ La, Lu, Nd, and Dy. In this contribution we will focus on the $Tb_5(Si_xGe_{1-x})_4$ series. The structural and magnetic properties of the parent compounds Tb_5Si_4 and Tb_5Ge_4 were reported over 30 years ago.[10] Tb_5Si_4 orders ferromagnetically at $T_C \cong 225$ K, and the basic physical properties, i.e., magnetization, susceptibility, specific heat, and resistivity, can be found elsewhere.[11,12] Tb_5Ge_4 orders in a complex canted-antiferromagnetic structure[13] at $T_N \cong 91$ K. In a previous contribution[14] we reported on the magnetocaloric effect in $Tb_5(Si_xGe_{1-x})_4$ with $x=0.0$, 0.5, and 1.0, as determined from magnetization measurements in magnetic fields up to 12 T. We found a previously unreported magnetic transition in Tb_5Ge_4 below the Néel temperature and a first-order paramagnetic to ferromagnetic transition in $Tb_5(Si_{0.5}Ge_{0.5})_4$. Furthermore, Spichkin *et al.*[12] also discovered a magnetic transition in Tb_5Si_4 below T_C that they associated with a spin reorientation transformation that could be related to ferromagnetic or noncollinear ordering of the Tb magnetic moments located in different crystallographic sites. Room-temperature crystal structure and magnetothermal properties of some $Tb_5(Si_xGe_{1-x})_4$ alloys with $x \geqslant 0.5$ have recently been reported by Huang *et al.*[15]

Despite the enormous current interest in the 5:4 compounds, the precise magnetic structures of these intriguing compounds remain largely unknown. To our knowledge, no comprehensive neutron diffraction study has been carried out, with the few exceptions of the R_5Ge_4 alloys with $R=$ Tb,[13] Ho,[16] and Nd.[17] We should note that it is not possible for us to investigate the most interesting and best studied $Gd_5(Si_xGe_{1-x})_4$ system due to the huge neutron absorption cross section of Gd. The aim of this work is to perform a neutron powder diffraction study of the $Tb_5(Si_xGe_{1-x})_4$ series as a function of both temperature and composition. As a main result, the magnetic and structural phase diagram has been determined.

II. EXPERIMENT

Polycrystalline samples of composition $Tb_5(Si_xGe_{1-x})_4$ ($x=1.0$, 0.8, 0.7, 0.6, 0.5, 0.4, 0.3, 0.2, and 0.0) have been synthesized by arc melting of 99.9 wt % pure Tb and 99.9999 wt % pure Si and Ge (all elements purchased from Alfa Aesar) under a high-purity argon atmosphere. Weight losses during melting were negligible, and therefore the initial composition was assumed unchanged. The quality of the as-cast samples was checked by room-temperature x-ray diffraction and scanning electron microscopy. The x-ray patterns con-

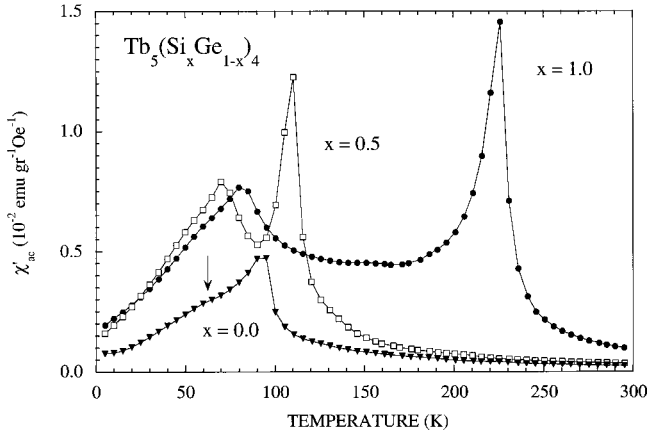

FIG. 1. ac magnetic susceptibility of some selected $Tb_5(Si_xGe_{1-x})_4$ alloys ($x=1.0$, 0.5, and 0) as a function of temperature. The arrow signals an additional magnetic transition in Tb_5Ge_4.

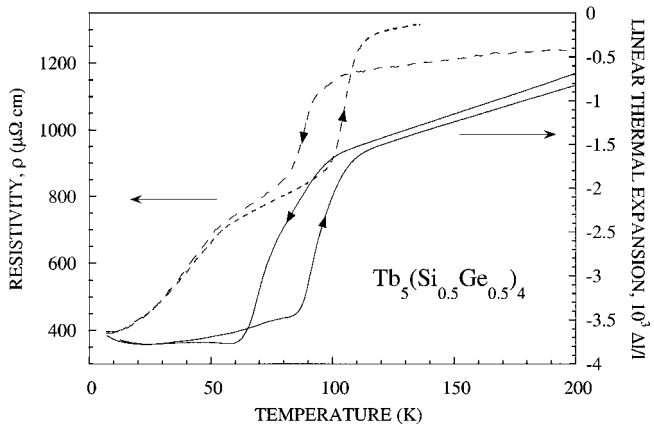

FIG. 2. Linear thermal expansion ($\Delta l/l$) and zero-field resistivity (ρ) of $Tb_5(Si_{0.5}Ge_{0.5})_4$ as a function of temperature.

firm the presence of an orthorhombic main phase (*Pnma*) for the compounds with compositions $x=1.0$, 0.8, 0.7, 0.3, 0.2, and 0.0. The $Tb_5(Si_xGe_{1-x})_4$ alloys with $x=0.6$, 0.5, and 0.4 crystallize in the monoclinic ($P112_1/a$) symmetry. The latter is similar to that found in some compositions of $R_5(Si_xGe_{1-x})_4$ with $R=$Gd,[1,3,4] Nd,[9] and Dy.[9] Minor amounts of secondary 5:3 and 1:1 phases have been detected in all samples except for $x=0.0$. X-ray Rietveld refinements yield values of ~5% (5:3) and ~10% (1:1), these being roughly constant (variations <1%) with x. Neutron Rietveld fits in the paramagnetic phase ($T=250$ K) and in $x=1.0$, 0.6, and 0.5 (see below) are in perfect agreement. No further thermal treatment has been carried out.

The ac magnetic susceptibility was measured using a commercial (Quantum Design) superconducting quantum interference device (SQUID) magnetometer with an excitation field of 1 Oe (peak value) at a frequency of 10 Hz.

Linear thermal expansion measurements were performed using the strain-gauge technique. The electrical resistivity experiments were done with a conventional four-probe method (excitation dc current of 5 mA).

Neutron diffraction experiments were carried out in $x=1.0$, 0.6, 0.5, and 0.0 on the high-resolution powder diffractometer D2B ($\lambda=1.596$ Å) and the high-intensity powder diffractometer D1B ($\lambda=2.52$ Å), both at the ILL, Grenoble. Diffraction patterns were collected between $2\theta=5°$ and 165° (D2B) at selected temperatures ranging from 2 to 300 K. The data were analyzed using the Rietveld refinement program FULLPROF,[18] which allows the simultaneous refinement of structural and magnetic profiles.

III. RESULTS FROM MACROSCOPIC MEASUREMENTS

ac initial magnetic susceptibility measurements have been carried out for all the $Tb_5(Si_xGe_{1-x})_4$ alloys as a function of temperature between 5 and 300 K. The results for some selected compositions ($x=1.0$,0.5,0.0) can be seen in Fig. 1. In all samples except the Ge-rich ones ($x=0.3$, 0.2, and $x=0.0$) a large peaklike anomaly signals the onset of magnetic order (ferromagnetism). The macroscopic ferro- or antiferromagnetic behavior below the ordering transitions was clearly established in the pure compounds (see the Introduction) and has been checked in all our samples by magnetization measurements (not reported here). Furthermore, a second low-temperature anomaly has been detected below T_C. Our results for Tb_5Si_4 are in perfect agreement with those reported recently.[12] In the monoclinic range of compositions ($x=0.4$, 0.5, and 0.6) the paramagnetic to ferromagnetic transition is of first order with a thermal hysteresis of ≈5 K (the measurement shown in Fig. 1 has been recorded upon increasing temperature). In the Ge-rich alloys (see, e.g., $x=0.0$ in Fig. 1) a smaller peak indicates the antiferromagnetic order. At lower temperatures (≈62 K) a change in slope is clearly visible (marked with an arrow in Fig. 1), suggesting a further change in the magnetic structure. Anomalies in the magnetocaloric effect at these low temperature transitions have been found in Tb_5Ge_4 (Ref. 14) and in $x=1.0$, 0.75, and 0.5 (Ref. 15). It is worth noting that an unusual behavior in the magnetocaloric effect has also been reported in the Dy_5Ge_4-based solid-solution region of $Dy_5(Si_xGe_{1-x})_4$,[19] suggesting a similar phenomenology. From the anomalies in the ac susceptibility we can delimit preliminary phase boundaries in the temperature-composition phase diagram. The different regions follow a similar pattern as that of the $Gd_5(Si_xGe_{1-x})_4$ system[2,5] with intermediate values of the ordering temperatures between those of the $R=$Gd and $R=$Dy series,[9] as expected from the different de Gennes factor $[(g_J-1)^2J(J+1)]$ of the specific R ion.

The magnetocaloric effect in $Tb_5(Si_{0.5}Ge_{0.5})_4$ is significantly larger than in the parent compounds (21.8 J/kg K in $\Delta H=5$ T, Ref. 6), suggesting that the first-order para- to ferromagnetic transition is associated with a structural transformation as in $Gd_5(Si_xGe_{1-x})_4$.[3–5] To further investigate this possibility, linear thermal expansion ($\Delta l/l$) and resistivity (ρ) measurements were performed as a function of temperature in the $x=0.5$ alloy, the results being displayed in Fig. 2. Large anomalies are observed at T_C, $\Delta l/l\cong 0.2\%$ and

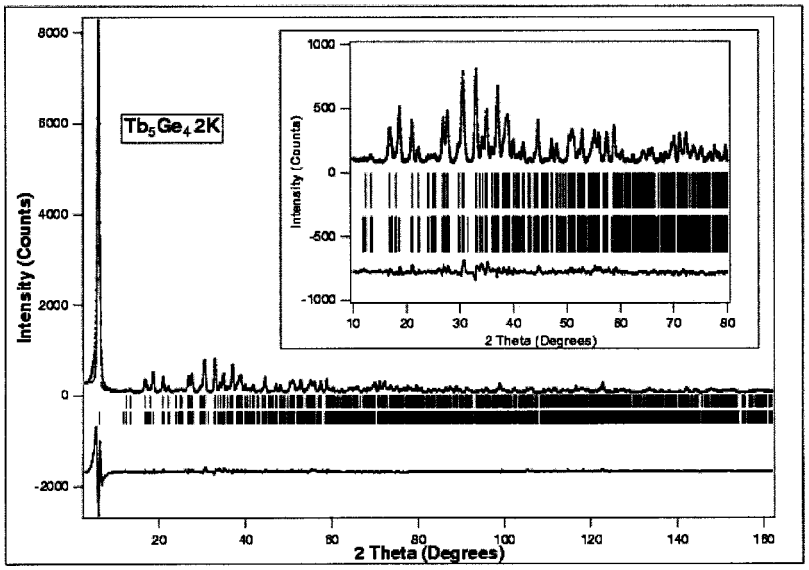

FIG. 3. Neutron diffraction pattern of Tb_5Ge_4 at 2 K (D2B). Dots are experimental data, and the lines show the calculated profile and residuals. The fit excluding the high-intensity low-angle magnetic reflection is shown in the inset up to 80°.

$\Delta\rho/\rho \cong 30\%$, the hysteresis emphasizes the first-order character of the transition. A similar behavior in both linear thermal expansion and resistivity has been observed in the $Gd_5(Si_xGe_{1-x})_4$ system,[3,5–7] pointing to an analogous physical origin of the first-order transitions observed in the monoclinic alloys.

Nevertheless, the $Tb_5(Si_xGe_{1-x})_4$ system presents several differences when compared with $Gd_5(Si_xGe_{1-x})_4$.[5] The first-order magnetostructural transition in the Ge-rich $Gd_5(Si_xGe_{1-x})_4$ alloys with $x \leqslant 0.2$ (see details in Ref. 5) has disappeared in the Tb compounds and is also absent in the Dy series.[19] Therefore, the presence of a magnetostructural transition seems limited to the intermediate composition range. In addition, a new phase boundary, missing in the Gd system, is now present at low temperatures in the $Tb_5(Si_xGe_{1-x})_4$ phase diagram. *A priori*, a change in the crystallographic structure at this low-temperature transition line cannot be ruled out.

IV. RESULTS FROM NEUTRON DIFFRACTION EXPERIMENTS

In order to get a deeper insight into the behavior of these complex compounds, a precise knowledge of both crystallographic and magnetic structure as a function of temperature is required. With that aim, we have performed neutron diffraction experiments in the compounds with concentrations $x = 0.0$, 0.5, 0.6, and 1.0, representatives of the different regions in the tentative phase diagram as determined from macroscopic measurements.

A. Tb_5Ge_4

High-resolution neutron diffraction spectra were collected on D2B at selected temperatures $T = 250$, 85, and 2 K. As an illustrative example, the neutron diffraction pattern of Tb_5Ge_4 at 2 K is shown in Fig. 3. A high-intensity asymmetric low-angle magnetic peak is clearly observed. We carried out the refinements with and without this reflection, the differences in the refined parameters being within the error bars (larger error bars were obtained for the lattice constants if included). We excluded this peak in the final refinement: see the inset of Fig. 3 (for clarity only data up to 80° have been plotted, but in the fit the whole angular range $2\theta = 10° - 160°$ is relevant). The Rietveld-refined lattice parameters, fractional atomic coordinates, and Tb magnetic moments are listed in Table I. We have confirmed that this compound crystallizes in the *Pnma* orthorhombic space group and that the atomic arrangement is the same as in the isomorphic Sm_5Ge_4 (Ref. 20) and Gd_5Ge_4 (Ref. 21) compounds. Both space group and precise atomic arrangement remain unaltered upon cooling down to 2 K.

The magnetic refinement at 2 K leads to a complex canted-antiferromagnetic structure which is schematically depicted in Fig. 4(a). The magnetic moments are essentially confined to the (a,c) plane, the main antiferromagnetic axis being along the c direction. The Tb1 ions (at $4c$: see Table I) form an almost collinear sublattice, the angle with the c axis is about 10°. The Tb2 and Tb3 (at $8d$: see Table I) canting angles with respect to c are larger, 23° and 31°, respectively. Our results are in very good agreement with a previous neutron diffraction study.[13] Following the notation in Ref. 13, this corresponds to the $Pnm'a$ magnetic space group with G_xA_z and $L_xP_yR_z$ magnetic modes for the $4c$ and $8d$ Tb positions, respectively. The relative signs of the different magnetic moments for the relevant magnetic modes in this work are reproduced in Table II. The refined components of the magnetic moments for all of the studied compounds can be found in Table III. The 85 K data have been refined using the same magnetic structure model. Nevertheless, the magnetic structure is now almost collinear, the Tb1, Tb2, and Tb3 ions making canting angles with respect to c of 0°, 7°, and 27°, respectively (angles with respect to an arbitrary direction can be obtained from the data in Table III). This structure is depicted in Fig. 4(b). The projection in the (a,c) plane has also been included to emphasize the canting of the Tb3 ions. Therefore, we can confirm the existence of a spin reorientation transition (T_{SR}) on cooling from the structure shown in Fig. 4(b) to that in Fig. 4(a).

TABLE I. Space group, lattice parameters, unit-cell volume, fractional atomic coordinates, Tb magnetic moments, and reliability factors (as defined in Ref. 18) of Tb_5Ge_4 at 250, 85, and 2 K, as refined from D2B neutron diffraction data. Numbers in parentheses indicate standard deviation of the last digit.

	250 K	85 K	2 K
Space group	*Pnma*	*Pnma*	*Pnma*
a (Å)	7.6373(3)	7.6308(3)	7.6303(3)
b (Å)	14.6997(6)	14.6738(6)	14.6809(5)
c (Å)	7.7159(3)	7.6994(3)	7.6934(3)
V (Å^3)	866.24(6)	862.12(6)	861.81(6)
Tb1 ($4c$):x	0.2890(9)	0.288(1)	0.2864(9)
y	$\frac{1}{4}$	$\frac{1}{4}$	$\frac{1}{4}$
z	0.0018(7)	−0.0002(9)	0.000(1)
Tb2 ($8d$):x	0.9741(5)	0.9709(6)	0.9670(5)
y	0.1012(2)	0.1017(3)	0.1016(3)
z	0.8221(5)	0.8220(7)	0.8236(7)
Tb3 ($8d$):x	0.1229(5)	0.1185(6)	0.1161(5)
y	0.1169(2)	0.1158(3)	0.1155(2)
z	0.3368(5)	0.3386(7)	0.3357(7)
Ge1 ($4c$):x	0.9161(7)	0.9114(8)	0.9101(9)
y	$\frac{1}{4}$	$\frac{1}{4}$	$\frac{1}{4}$
z	0.1142(7)	0.1123(8)	0.1123(9)
Ge2 ($4c$):x	0.1700(6)	0.1686(7)	0.1672(8)
y	$\frac{1}{4}$	$\frac{1}{4}$	$\frac{1}{4}$
z	0.6361(7)	0.6360(8)	0.6355(9)
Ge3 ($8d$):x	0.2200(5)	0.2222(6)	0.2235(7)
y	0.9562(2)	0.9561(3)	0.9560(3)
z	0.5316(5)	0.5274(6)	0.5265(6)
μ_{Tb1} (μ_B)		4.57(9)	8.5(1)
μ_{Tb2} (μ_B)		3.1(1)	7.7(1)
μ_{Tb3} (μ_B)		3.7(1)	8.7(1)
R_p/R_{wp} (%)	3.8/4.6	4.5/5.9	6.0/8.0
R_{Bragg} (%)	8.7	10.4	14
R_{mag} (%)		5.6	6.3
χ^2	1.4	2.7	4.2

In order to determine T_{SR} more precisely, we have performed a continuous scan over the range 2–100 K on the high-intensity D1B instrument. In Figs. 5(a) and 5(b) we display the temperature dependence of the intensity of the (010) and (102)+(201) lines. From the thermal evolution of the (010) intensity, the disappearance of the antiferromagnetic order at T_N can be clearly noticed: see Fig. 5(a). The intensity of this purely magnetic superstructure line only depends on the component of the magnetic moments along c, and therefore, T_{SR} cannot be detected. In contrast, the magnetic moment components along a and b do contribute to the intensity of the (102)+(201) lines, and as can be seen in Fig. 5(b), T_{SR} is clearly detected at ≈55 K, in very good agreement with the anomalies seen in the ac susceptibility (see Fig. 1) and the MCE.[14]

B. Tb_5Si_4

No previous information is available in the magnetic structures as a function of temperature of the rest of the

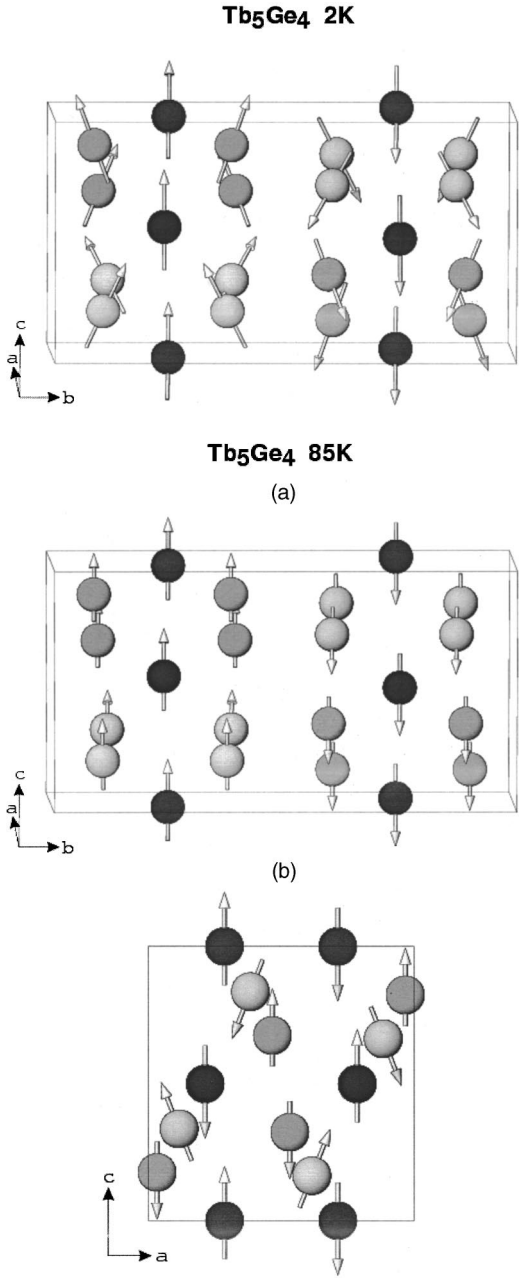

FIG. 4. Schematic representation of the magnetic structures of Tb_5Ge_4 at 2 K (a) and 85 K (b) as determined from the Rietveld refinement of the high-resolution D2B neutron powder diffraction data. The spheres represent Tb ions, and a different level of shading is used to identify Tb1 (black), Tb2 (medium gray), and Tb3 (lightest gray). The projection in the (a,c) plane has also been included in (b) to emphasize the canting of the Tb3 ions.

$Tb_5(Si_xGe_{1-x})_4$ series, including the parent alloy Tb_5Si_4, which has been well studied by using macroscopic techniques as mentioned before.[10–12,14,15] Neutron powder diffraction spectra were collected on D2B at selected temperatures of 250, 85, and 2 K. The lattice parameters, fractional atomic coordinates, and Tb magnetic moments from our Rietveld refinements are listed in Table IV. We have confirmed that this compound crystallizes at high temperature in the *Pnma* orthorhombic space group with a Gd_5Si_4-type

TABLE II. The different magnetic modes of the nonequivalent symmetry positions $4c$ and $8d$ for the three relevant (in this work) magnetic space groups of *Pnma* associated with the magnetic propagation vector, $\mathbf{q}=0$ (Ref. 13).

		$Pnm'a$			$Pnm'a'$			$Pn'm'a$		
i	Position $4c$	G_x		A_z	F_x		C_z	C_x		F_z
1		+		+	+		+	+		+
2		−		−	+		+	+		+
3		+		−	+		−	−		+
4		−		+	+		−	−		+
	$8d$	L_x	P_y	R_z	F_{Bx}	A_{By}	G_{Bz}	G_{Bx}	C_{By}	F_{Bz}
1		+	+	+	+	+	+	+	+	+
2		−	+	+	+	−	−	−	+	+
3		−	+	−	+	−	+	+	−	+
4		+	+	−	+	+	−	−	−	+
5		−	−	−	+	+	+	+	+	+
6		+	−	−	+	−	−	−	+	+
7		+	−	+	+	−	+	+	−	+
8		−	−	+	+	+	−	−	−	+

atomic arrangement[21,22] as reported previously.[12,15] No crystallographic transformation has been detected down to 2 K.

The magnetic structure in the ferromagnetic phase has been determined at 85 K to be a complex arrangement of canted spins described in the magnetic space group $Pnm'a'$ with F_xC_z and $F_{Bx}A_{By}G_{Bz}$ magnetic modes for the $4c$ and $8d$ Tb positions, respectively (Table II). The schematic arrangement of the Tb magnetic moments is depicted in Fig. 6(a). The *a* axis is the main (easy) ferromagnetic direction. The canting angles with respect to the *a* axis are, for Tb1, Tb2, and Tb3 (see Table IV), 3°, 17°, and 4°, respectively. At the lowest measured temperature of 2 K the magnetic structure has changed. A second strong ferromagnetic coupling develops along the *c* axis, and the refinement reveals that the magnetic structure comprises a mixing of two magnetic modes: $Pnm'a'$ with F_xC_z and $F_{Bx}A_{By}G_{Bz}$ as at 85 K and $Pn'm'a$ with C_xF_z and $G_{Bx}C_{By}F_{Bz}$ ($4c$ and $8d$, respectively) magnetic modes: see Tables II and III. This magnetic structure is displayed in Fig. 6(b). Due to the magnetic mode mixing, the sets of magnetic Tb ions on $4c$ and $8d$ positions get split into 2×2 ($4c$) and 2×4 ($8d$) subsets. Tables III and IV list the corresponding magnetic moment values at 2 K for the two sets of Tb1, Tb2, and Tb3 positions. The averaged (over the two subsets) canting angles for Tb1, Tb2, and Tb3 with respect to the *c* axis are 57°, 45°, and 56°, respectively. At 2 K, the magnetic moments for Tb are slightly larger than the $9\mu_B$ expected theoretically for Tb. The magnetic ordering of the 5:3 and 1:1 impurity phases at low temperatures makes the fitting procedure complicated (the first large magnetic reflection of the 5:3 phase had to be excluded), leading to large error bars in the determined magnetic moment values.

TABLE III. Components of the Tb magnetic moments for all of the studied $Tb_5(Si_xGe_{1-x})_4$ compounds as determined form the Rietveld refinements of the D2B neutron powder diffraction data. The corresponding crystallographic information can be found in Tables I, IV, V, and VI.

		μ_{Tb1} (μ_B)			μ_{Tb2} (μ_B)			μ_{Tb3} (μ_B)		
x	T (K)	μ_x	μ_y	μ_z	μ_x	μ_y	μ_z	μ_x	μ_y	μ_z
0.0	85	0	0	4.57(9)	0.3(2)	0.2(2)	3.0(1)	1.3(2)	1.0(2)	3.3(1)
	2	1.49(8)	0	8.3(1)	2.7(1)	1.5(1)	7.06(8)	4.1(1)	1.8(1)	7.49(9)
1.0	85	8.38(8)	0	0.4(1)	7.45(7)	1.25(8)	1.91(5)	8.09(7)	0.07(8)	0.62(6)
	2	8.3(3)	0	4.7(2)	5.9(3)	0.5(1)	7.7(2)	7.5(2)	0.4(2)	5.2(2)
		7.8(2)	0	5.9(3)	6.8(3)	4.2(1)	6.3(2)	8.8(2)	0.2(2)	5.7(2)
0.5	100	8.51(9)	0	0.8(1)	7.20(8)	1.5(1)	1.26(8)	7.63(8)	0.4(1)	0.2(1)
	85	8.50(8)	0	0.7(1)	7.45(7)	1.54(8)	1.76(6)	8.04(7)	0.67(9)	0.40(8)
	2	9.3(3)	0	3.7(2)	7.2(3)	0.1(1)	7.0(2)	8.7(2)	0.0(2)	5.6(2)
		7.7(3)	0	5.1(3)	6.6(3)	4.3(2)	5.4(2)	8.2(2)	1.0(2)	3.7(2)
0.6	85	8.49(8)	0	0.8(1)	7.45(7)	1.1(1)	1.72(6)	7.94(7)	0.4(1)	0.44(8)

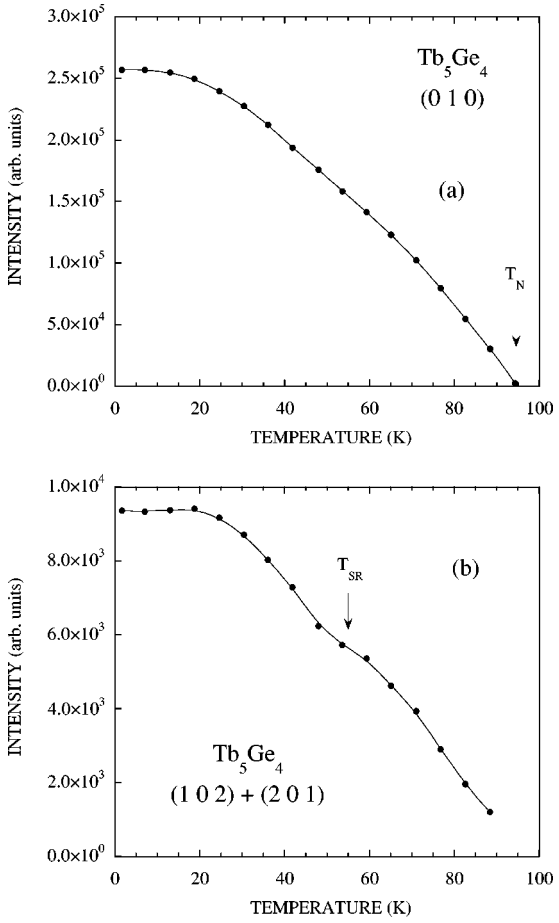

FIG. 5. Temperature dependence of the intensity of the (010) (a) and (102)+(201) (b) diffraction peaks of Tb_5Ge_4 as determined from D1B data. The onset of the antiferromagnetic order (T_N) and the spin reorientation transition (T_{SR}) have been indicated.

In order to follow more precisely the onset of this low-temperature magnetic transition, we show in Fig. 7 the thermal evolution of the intensity of several selected lines as determined from D1B data. The (131) peak shows a nearly normal, slowly increasing behavior as the magnetic moments increase with decreasing temperature. The change in the magnetic structure is, however, evident from the temperature dependence of the (100)+(020) magnetic line at $T_C' \approx 80$ K. The decrease seen at T_C' is determined by the (100) peak which loses its intensity as the coupling in the *c* direction changes from antiferromagnetic to ferromagnetic. The (040) peak possesses no intensity coming from the antiferromagnetic coupling along *c* and shows no inflection at T_C'. This reflection increases, however, still strongly below T_C' as the antiferromagnetic component is turning into a ferromagnetic one. Therefore, our study demonstrates that the low-temperature peak in the ac susceptibility first and recently reported by Spichkin *et al.*[12] (see also Fig. 1) is indeed a second magnetic phase transition between the structures depicted in Figs. 6(a) and 6(b).

C. $Tb_5(Si_{0.5}Ge_{0.5})_4$ and $Tb_5(Si_{0.6}Ge_{0.4})_4$

As already discussed in Sec. III, the behavior of $\Delta l/l$, ρ (Fig. 2), and the large MCE (Ref. 14) of $Tb_5(Si_{0.5}Ge_{0.5})_4$ in the vicinity of T_C suggests that this transition is similar in origin to that found in the $Gd_5(Si_xGe_{1-x})_4$ alloys with $0.24 \leqslant x \leqslant 0.5$.[3,4] To further investigate this point and to determine the magnetic structure at low temperatures, we recorded D2B neutron diffraction spectra at selected temperatures $T=250$, 100, 85, and 2 K. We also measured the $Tb_5(Si_{0.6}Ge_{0.4})_4$ alloy at 250 and 85 K, which behaves macroscopically similarly to $x=0.5$. The refined structural and magnetic parameters are collected in Tables V, VI, and III. At 250 K these two compounds crystallize in the $P112_1/a$ monoclinic space group, the precise atomic arrangement being as in the monoclinic $Gd_5(Si_xGe_{1-x})_4$ alloys.[21] Upon cooling, both $x=0.5$ and 0.6 alloys experience a first-order structural transition to a *Pnma* orthorhombic symmetry and we have confirmed that the atomic arrangement is identical to that found in Tb_5Si_4 (Sec. IV B). At this transition, abrupt changes in the cell parameters take place, the most dramatic change being along the *a* axis. For example, from the data in Table V for $x=0.5$, we can estimate a change on cooling of -0.99%,

TABLE IV. Space group, lattice parameters, unit-cell volume, fractional atomic coordinates, Tb magnetic moments, and reliability factors (as defined in Ref. 18) of Tb_5Si_4 at 250, 85, and 2 K, as refined from D2B neutron diffraction data. Numbers in parentheses indicate standard deviation of the last digit.

	250 K	85 K	2 K
Space group	*Pnma*	*Pnma*	*Pnma*
a (Å)	7.4076(2)	7.4013(2)	7.4031(2)
b (Å)	14.5950(4)	14.5834(4)	14.5816(4)
c (Å)	7.6879(2)	7.6694(2)	7.6623(2)
V (Å^3)	831.18(4)	827.80(4)	827.13(4)
Tb1 ($4c$):x	0.3520(6)	0.3531(4)	0.3551(4)
y	$\frac{1}{4}$	$\frac{1}{4}$	$\frac{1}{4}$
z	$-0.0148(6)$	$-0.0115(3)$	$-0.0111(4)$
Tb2 ($8d$):x	0.0275(4)	0.0279(3)	0.0276(2)
y	0.0976(2)	0.0969(1)	0.0967(1)
z	0.8191(4)	0.8180(2)	0.8160(3)
Tb3 ($8d$):x	0.1822(4)	0.1810(3)	0.1825(3)
y	0.1227(2)	0.1225(1)	0.1231(1)
z	0.3216(4)	0.3228(2)	0.3216(2)
Si1 ($4c$):x	0.981(1)	0.979(1)	0.976(1)
y	$\frac{1}{4}$	$\frac{1}{4}$	$\frac{1}{4}$
z	0.102(1)	0.098(1)	0.098(1)
Si2 ($4c$):x	0.236(1)	0.239(1)	0.236(2)
y	$\frac{1}{4}$	$\frac{1}{4}$	$\frac{1}{4}$
z	0.624(1)	0.627(1)	0.623(1)
Si3 ($8d$):x	0.1461(9)	0.145(1)	0.147(1)
y	0.9598(4)	0.9595(4)	0.9583(5)
z	0.5263(8)	0.5255(9)	0.526(1)
μ_{Tb1} (μ_B)		8.39(8)	9.5(2)/9.7(2)
μ_{Tb2} (μ_B)		7.79(7)	9.7(2)/10.2(2)
μ_{Tb3} (μ_B)		8.12(7)	9.1(2)/10.5(2)
R_p/R_{wp} (%)	2.8/3.4	3.6/4.4	3.8/4.9
R_{Bragg} (%)	7.9	5.0	4.3
R_{mag} (%)		5.6	3.8
χ^2	1.6	2.3	2.9

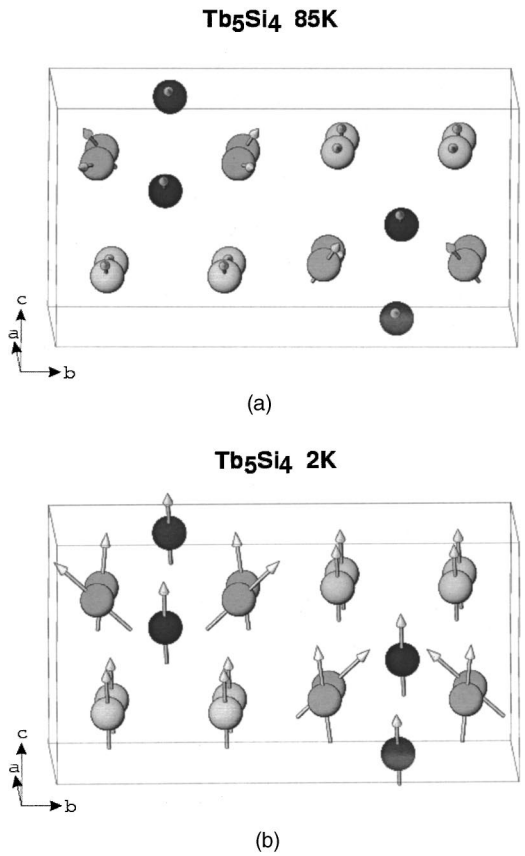

FIG. 6. Schematic representation of the magnetic structures of Tb_5Si_4 at 85 K (a) and 2 K (b) as determined from the Rietveld refinement of the high-resolution D2B neutron powder diffraction data. The spheres represent Tb ions and a different level of shading is used to identify Tb1 (black), Tb2 (medium gray), and Tb3 (lightest gray).

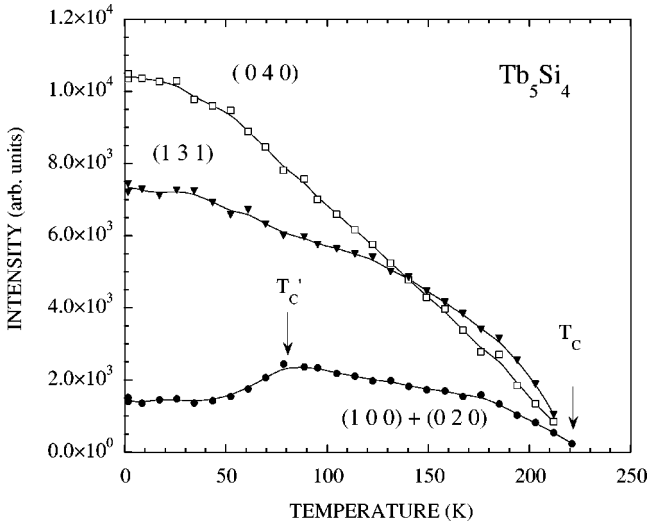

FIG. 7. Temperature dependence of the intensity of some selected diffraction peaks of Tb_5Si_4 as determined from D1B data. The onset of the ferromagnetic order (T_C) and the second magnetic phase transition (T_C') have been indicated.

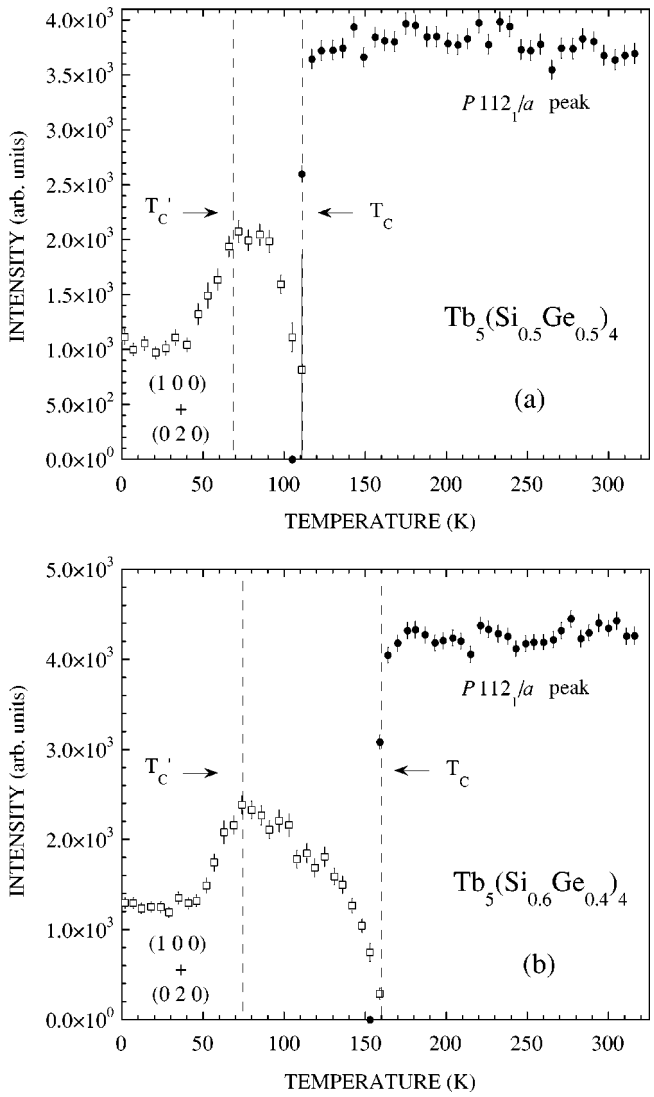

FIG. 8. Temperature dependence of the intensity of a selected structural monoclinic ($P112_1/a$) diffraction peak (●) and the purely magnetic (100)+(020) reflection (□) of $Tb_5(Si_{0.5}Ge_{0.5})_4$ (a) and $Tb_5(Si_{0.6}Ge_{0.4})_4$ (b) as determined from D1B data. The onset of the ferromagnetic order (T_C) and the additional low-temperature magnetic phase transition (T_C') have been indicated.

-0.16%, and $+0.07\%$ along a, b, and c, respectively. If we correct $\approx -0.15\%$ for the linear thermal expansion as determined above T_C (see Fig. 2), we obtain more reliable final values of $\Delta a/a \approx -0.84\%$, $\Delta b/b \approx -0.01\%$, and $\Delta c/c \approx +0.22\%$. The volume change $\Delta V/V \approx -0.5\%$ is in good agreement with that found from our linear thermal expansion measurements, $3(\Delta l/l) \approx -0.6\%$ (Fig. 2), taking into consideration the approximations made and possible texture effects. These values are similar to those found in $Gd_5(Si_{0.5}Ge_{0.5})_4$ (Ref. 4) and in a close composition, $x = 0.45$ (Ref. 3).

The magnetic structure at 100 and 85 K in $x = 0.5$ and at 85 K in $x = 0.6$ is identical to that found in Tb_5Si_4 at 85 K, i.e., $Pnm'a'$ with the couplings indicated in Table II: see also Fig. 6(a). It is interesting to note that at 100 K (only some 10 K below T_C) in $x = 0.5$ (Table V) the magnetic mo-

TABLE V. Space group, lattice parameters, unit-cell volume, fractional atomic coordinates, Tb magnetic moments, and reliability factors (as defined in Ref. 18) of $Tb_5(Si_{0.5}Ge_{0.5})_4$ at 250, 100, 85, and 2 K, as refined from D2B neutron diffraction data. Numbers in parentheses indicate standard deviation of the last digit. $M = 0.5Si + 0.5Ge$.

	250 K		100 K	85 K	2 K
Space group	$P112_1/a$		*Pnma*	*Pnma*	*Pnma*
a (Å)	7.5080(5)		7.4340(3)	7.4313(2)	7.4322(3)
b (Å)	14.652(1)		14.6290(6)	14.6278(5)	14.6280(5)
c (Å)	7.7117(5)		7.7171(3)	7.7151(3)	7.7082(3)
γ (deg)	93.042(5)				
V (Å^3)	847.1(1)		839.25(6)	838.66(5)	838.03(5)
Tb1 $(4e)$:x	0.324(1)	Tb1 $(4c)$:x	0.3476(6)	0.3473(5)	0.3460(5)
y	0.2466(6)	y	$\frac{1}{4}$	$\frac{1}{4}$	$\frac{1}{4}$
z	0.0033(9)	z	−0.0099(4)	−0.0104(4)	−0.0093(4)
Tb2A $(4e)$:x	−0.000(1)	Tb2 $(8d)$:x	0.0202(4)	0.0205(3)	0.0210(3)
y	0.0994(5)	y	0.0966(1)	0.0968(1)	0.0971(1)
z	0.179(1)	z	0.8192(4)	0.8180(3)	0.8178(3)
Tb2B $(4e)$:x	0.019(1)				
y	0.4002(5)				
z	0.182(1)				
Tb3A $(4e)$:x	0.359(1)	Tb3 $(8d)$:x	0.1763(4)	0.1765(3)	0.1774(3)
y	0.8820(5)	y	0.1227(2)	0.1229(1)	0.1230(1)
z	0.168(1)	z	0.3217(3)	0.3224(3)	0.3220(3)
Tb3B $(4e)$:x	0.331(1)				
y	0.6199(5)				
z	0.176(1)				
$M1$ $(4e)$:x	0.953(1)	$M1$ $(4c)$:x	0.977(1)	0.976(1)	0.979(1)
y	0.2522(6)	y	$\frac{1}{4}$	$\frac{1}{4}$	$\frac{1}{4}$
z	0.893(1)	z	0.1047(9)	0.103(8)	0.1045(9)
$M2$ $(4e)$:x	0.207(1)	$M2$ $(4c)$:x	0.227(1)	0.2274(9)	0.227(1)
y	0.2528(6)	y	$\frac{1}{4}$	$\frac{1}{4}$	$\frac{1}{4}$
z	0.366(1)	z	0.634(1)	0.6321(9)	0.632(1)
$M3A$ $(4e)$:x	0.206(1)	$M3$ $(8d)$:x	0.1537(9)	0.1548(8)	0.1552(8)
y	0.9581(6)	y	0.9597(4)	0.9595(3)	0.9587(4)
z	0.469(1)	z	0.5299(7)	0.5300(7)	0.5301(7)
$M3B$ $(4e)$:x	0.153(1)				
y	0.5435(6)				
z	0.466(1)				
μ_{Tb1} (μ_B)			8.5(1)	8.53(9)	9.2(2)/10.0(2)
μ_{Tb2} (μ_B)			7.65(8)	7.81(7)	9.6(2)/10.1(2)
μ_{Tb3} (μ_B)			7.47(8)	8.08(7)	9.1(2)/10.3(2)
R_p/R_{wp} (%)	2.6/3.2		3.6/4.4	3.5/4.4	3.7/4.6
R_{Bragg} (%)	6.3		6.2	5.4	4.0
R_{mag} (%)			5.6	4.6	3.2
χ^2	1.4		2.6	2.5	2.9

ment values are already very high, in good agreement with the first-order character of the magnetostructural transition. The refinement at 2 K in $x=0.5$ leads again to the same mainly ferromagnetic structure as found in Tb_5Si_4, Fig. 6(b), indicating a common structural and magnetic ground state.

In Figs. 8(a) and 8(b) we show the temperature dependence of the intensity of a monoclinic ($P112_1/a$) peak and the purely magnetic line (100)+(020) in the range 320 K $>T>$2 K for $x=0.5$ (a) and $x=0.6$ (b) (D1B data). As can be seen in Figs. 8(a) and 8(b), the disappearance of the intensity of the $P112_1/a$ reflection, which signals the structural transformation to the *Pnma* structure, is concomitant with the onset of the ferromagnetic order. These results represent complementary evidence that the crystallographic and magnetic degrees of freedom are completely coupled in the $R_5(Si_xGe_{1-x})_4$ compounds that exhibit first-order magnetostructural transitions. Also, the existence of a second low-temperature magnetic phase transition at T_C' similar to that

TABLE VI. Space group, lattice parameters, unit-cell volume, fractional atomic coordinates, Tb magnetic moments, and reliability factors (as defined in Ref. 18) of $Tb_5(Si_{0.6}Ge_{0.4})_4$ at 250 and 85 K, as refined from D2B neutron diffraction data. Numbers in parentheses indicate standard deviation of the last digit. $M = 0.6Si + 0.4Ge$.

	250 K		85 K
Space group	$P112_1/a$		*Pnma*
a (Å)	7.4980(5)		7.4253(2)
b (Å)	14.645(1)		14.6193(4)
c (Å)	7.7063(5)		7.7082(3)
γ (deg)	93.019(5)		
V (Å^3)	845.04(9)		836.74(5)
Tb1 ($4e$):x	0.323(1)	Tb1 ($4c$):x	0.3505(5)
y	0.2470(6)	y	$\frac{1}{4}$
z	0.0045(9)	z	−0.0119(3)
Tb 2A($4e$):x	0.001(1)	Tb2 ($8d$):x	0.0238(3)
y	0.0989(5)	y	0.0968(1)
z	0.180(1)	z	0.8189(3)
Tb2B ($4e$):x	0.022(1)		
y	0.3994(5)		
z	0.182(1)		
Tb3A ($4e$):x	0.354(1)	Tb3 ($8d$):x	0.1776(3)
y	0.8813(5)	y	0.1229(1)
z	0.170(1)	z	0.3224(9)
Tb3B ($4e$):x	0.331(1)		
y	0.6200(5)		
z	0.176(1)		
$M1$($4e$):x	0.951(1)	$M1$($4c$):x	0.978(1)
y	0.2517(7)	y	$\frac{1}{4}$
z	0.893(1)	z	0.1017(9)
$M2$($4e$):x	0.206(1)	$M2$($4c$):x	0.231(1)
y	0.2533(7)	y	$\frac{1}{4}$
z	0.363(1)	z	0.6299(9)
$M3A$($4e$):x	0.207(1)	$M3$($8d$):x	0.1545(8)
y	0.9566(7)	y	0.9599(3)
z	0.470(1)	z	0.5298(7)
$M3B$($4e$):x	0.150(1)		
y	0.5412(7)		
z	0.468(1)		
$\mu_{Tb1}(\mu_B)$			8.52(9)
$\mu_{Tb2}(\mu_B)$			7.72(7)
$\mu_{Tb3}(\mu_B)$			7.97(7)
R_p/R_{wp} (%)	3.1/3.9		3.9/4.9
R_{Bragg} (%)	7.9		5.2
R_{mag} (%)			5.7
χ^2	1.3		2.0

found in Tb_5Si_4 is clearly detected. The transition temperatures are in perfect agreement with our ac susceptibility results (Sec. III, Figs. 1 and 9).

V. DISCUSSION: MAGNETIC-STRUCTURAL PHASE DIAGRAM

From our macroscopic (mainly ac susceptibility) and microscopic neutron diffraction experiments, we have elaborated the magnetic and crystallographic temperature-composition phase diagram of the $Tb_5(Si_xGe_{1-x})_4$ materials, Fig. 9. We should compare this with the equivalent for the $Gd_5(Si_xGe_{1-x})_4$ materials.[5] As in the Gd alloys, we observe three different crystallographic structures at room temperature: O(I) (orthorhombic *Pnma* Gd_5Si_4 type), M (monoclinic $P112_1/a$), and O(II) (orthorhombic *Pnma* Gd_5Ge_4 type).[5,21] Upon lowering the temperature, long-range magnetic order sets in through a second-order transition (high-temperature dotted line in Fig. 9) either to a complex ferromagnetic structure in the case of the Si-rich alloys, FM1 [Fig. 6(a)], or to an antiferromagnetic structure for the Ge-rich region, AFM1 [Fig. 4(b)], without changes in the crystallographic structure. For the M alloys, a first-order magnetostructural transition to the FM1-O(I) state takes place (solid line in Fig. 9). These high-temperature transition boundaries correspond to those found in the $Gd_5(Si_xGe_{1-x})_4$ system.[5] On further cooling down, a second magnetic transition without a change in the crystallographic structure takes place in all the compounds, either via a spin reorientation to the AFM2 structure in the Ge-rich region [Fig. 4(a)] or via a magnetic mode mixing to the FM2 [Fig. 6(b)] for the rest of the composition range (open symbols, dotted line in Fig. 9). This low-temperature magnetic phase boundary is absent in the $Gd_5(Si_xGe_{1-x})_4$ alloys.[5] The precise relationships between atomic bonding, crystallographic structure, and magnetic interactions in the $Gd_5(Si_xGe_{1-x})_4$ system has been excellently reviewed in Ref. 23.

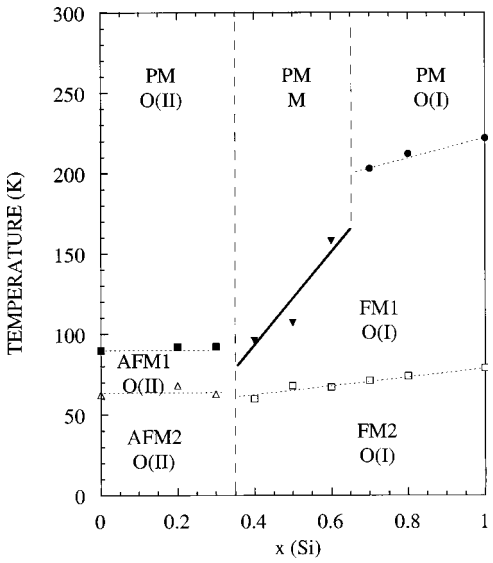

FIG. 9. Magnetic and crystallographic temperature-composition phase diagram of the $Tb_5(Si_xGe_{1-x})_4$ materials. PM, FM1, FM2, AFM1, and AFM2 label different magnetic phases and O(I), M, and O(II) denote different crystallographic structures, as defined throughout the text (see Sec. V). The transition temperatures have been taken from the anomalies in the ac susceptibility data. The solid line is a first-order magnetostructural phase boundary. Different symbols are used for different phase transitions.

VI. SUMMARY

In summary, we have carried out a detailed study of the crystallographic and magnetic structures of the

$Tb_5(Si_xGe_{1-x})_4$ system by means of macroscopic and microscopic techniques. From our results, the following conclusions can be drawn.

(i) The complex magnetic and crystallographic temperature-composition phase diagram of the $Tb_5(Si_xGe_{1-x})_4$ materials has been determined (Fig. 9). The use of neutron diffraction experiments has been indispensable to fully characterize the different crystallographic and magnetic phases as a function of temperature.

(ii) In Tb_5Ge_4, we have found that the anomalies observed in the ac susceptibility (see Fig. 1) and the anomalous behavior in the MCE reported earlier[14] have their origin in a spin reorientation transition between the canted-antiferromagnetic structures depicted in Figs. 4(a) and 4(b). No structural changes have been detected down to 2 K.

(iii) Tb_5Si_4 has been recently reported[12] to exhibit a second magnetic transition below T_C: see also Fig. 1. Our study demonstrates that there is indeed a magnetic phase transition between the structures depicted in Figs. 6(a) and 6(b). As in Tb_5Ge_4, no structural changes have been detected down to 2 K.

(iv) Alloys with intermediate compositions ($x=0.4$, 0.5, and 0.6) present a monoclinic ($P112_1/a$) structure at room temperature. On cooling down, these materials exhibit a first-order crystallographic-magnetic transformation to an orthorhombic $[O(\mathrm{I})]$ canted ferromagnetic (FM1) structure (see Fig. 9). These experimental results confirm the strong coupling between crystallographic and magnetic degrees of freedom in the $Tb_5(Si_xGe_{1-x})_4$ compounds. As in Tb_5Si_4, a second magnetic phase transition (FM1-FM2: see Fig. 9) without a change in the crystallographic structure has also been found.

ACKNOWLEDGMENTS

The financial support of the Spanish CICYT under Grant Nos. MAT99-1063-C04 and MAT2000-1756 is acknowledged.

*Corresponding author. FAX: 34-976-761229. Electronic address: morellon@posta.unizar.es

[1] V. K. Pecharsky and K. A. Gschneidner, Jr., Phys. Rev. Lett. **78**, 4494 (1997).
[2] V. K. Pecharsky and K. A. Gschneidner, Jr., Appl. Phys. Lett. **70**, 3299 (1997); V. K. Pecharsky and K. A. Gschneidner, Jr., J. Magn. Magn. Mater. **167**, L179 (1997).
[3] L. Morellon, P. A. Algarabel, M. R. Ibarra, J. Blasco, B. García-Landa, Z. Arnold, and F. Albertini, Phys. Rev. B **58**, R14 721 (1998).
[4] W. Choe, V. K. Pecharsky, A. O. Pecharsky, K. A. Gschneidner, Jr., V. G. Young, Jr., and G. J. Miller, Phys. Rev. Lett. **84**, 4617 (2000).
[5] L. Morellon, J. Blasco, P. A. Algarabel, and M. R. Ibarra, Phys. Rev. B **62**, 1022 (2000).
[6] L. Morellon, J. Stankiewicz, B. García-Landa, P. A. Algarabel, and M. R. Ibarra, Appl. Phys. Lett. **73**, 3462 (1998); L. Morellon, P. A. Algarabel, C. Magen, and M. R. Ibarra, J. Magn. Magn. Mater. **237**, 119 (2001).
[7] E. M. Levin, V. K. Pecharsky, and K. A. Gschneidner, Jr., Phys. Rev. B **60**, 7993 (1999); E. M. Levin, A. O. Pecharsky, V. K. Pecharsky, and K. A. Gschneidner, Jr., *ibid.* **63**, 064426 (2001).
[8] E. M. Levin, V. K. Pecharsky, and K. A. Gschneidner, Jr., Phys. Rev. B **63**, 174110 (2001).
[9] K. A. Gschneidner, Jr., V. K. Pecharsky, A. O. Pecharsky, V. V. Ivtchenko, and E. M. Levin, J. Alloys Compd. **303–304**, 214 (2000).
[10] F. Holtzberg, R. J. Gambino, and T. R. McGuire, J. Phys. Chem. Solids **28**, 2283 (1967).
[11] Yu. V. Serdyuk, R. P. Krentsis, and P. V. Gel'd, Sov. Phys. Solid State **23**, 1592 (1982).
[12] Y. I. Spichkin, V. K. Pecharsky, and K. A. Gschneidner, Jr., J. Appl. Phys. **89**, 1738 (2001).
[13] P. Schobinger-Papamantellos, J. Phys. Chem. Solids **39**, 197 (1978).
[14] L. Morellon, C. Magen, P. A. Algarabel, M. R. Ibarra, and C. Ritter, Appl. Phys. Lett. **79**, 1318 (2001).
[15] H. Huang, A. O. Pecharsky, V. K. Pecharsky, and K. A. Gschneidner, Jr. (private communication).
[16] P. Schobinger-Papamantellos and A. Niggli, J. Phys. (Paris), Colloq. **40**, C5-156 (1979).
[17] P. Schobinger-Papamantellos and A. Niggli, J. Phys. Chem. Solids **42**, 583 (1981).
[18] J. Rodríguez-Carvajal, Physica B **192**, 55 (1993); J. L. Rodriguez-Carvajal and T. Roisnel, http://www-llb.cea.fr/fullweb/fullprof.98/fp98.htm
[19] V. V. Ivtchenko, V. K. Pecharsky, and K. A. Gschneidner, Jr., Adv. Cryog. Eng. **46**, 405 (2000).
[20] G. S. Smith, Q. Johnson, and A. G. Tharp, Acta Crystallogr. **22**, 269 (1967).
[21] V. K. Pecharsky, and K. A. Gschneidner, Jr., J. Alloys Compd. **260**, 98 (1997).
[22] J. E. Iglesias and H. Steinfink, J. Less-Common Met. **26**, 45 (1972).
[23] V. K. Pecharsky and K. A. Gschneidner, Jr., Adv. Mater. **13**, 683 (2001).